1976 Summer Student Lecture Interstellar Masers

Some History

Shklovskii (1949) predicted that interstellar OH ought to be observable through absorption by the ground-state Λ-doublet of background continuum sources. Unfortunately, his frequencies were wrong by almost a factor of two. Weinreb et al. (1963), using the laboratory measurements of Ehrenstein et al. (1959) [4 transitions, at 1612, 1665, 1667, and 1720 MHz, with relative line strengths 1:5:9:1], made the first astronomical detection towards Cas A. It was found almost immediately that the relative intensities of the different OH transitions, particularly towards Sgr A, were not as expected from LTE. While the data could be fit assuming clumps of moderate optical depth, Gardner et al. (1964) noted that "an alternate explanation, such as perturbations of the populations of the [energy] levels, cannot be excluded".

Gundermann (1965) (working with Goldstein) and Weaver et al. (1965) independently, and almost simultaneously, found strong emission lines at the OH frequencies towards the HII region W49. Because they only saw the strong emission at 1665 MHz, Weaver

et al. attributed it to an unknown emitter, "mysterium", that was probably not OH. They noted with surprise that the narrow linewidths implied kinetic temperatures much smaller than those of the HII region with which they were associated. Gundermann (1965) and Weinreb et al. (1965), however, detected the strong emission at other OH frequencies, and correctly identified it as "anomalously excited OH". Weinreb et al. noted that some of the 1665 emission was as much as 37% linearly polarized. Davies et al. (1966) found that the lines were circularly polarized; invoking the Zeeman effect, they deduced magnetic fields ~ milligauss. Barrett and Rogers (1966) found the circular polarization independently. They noted that the velocity structure of the observed emission is so complex that the interpretation of specific features as Zeeman patterns was hazardous. [This is still true.] More importantly, their upper limit to the source size in W3 (OH) implied line brightness temperatures >2000°K, while the linewidths (if interpreted as thermal broadening) implied kinetic temperatures <50°K. From the fact that the lines were intense but narrow, Barrett and

Rogers inferred that they were in maser emission. They considered that the anomalous hyperfine intensity ratios and polarization supported this interpretation, because it is easy to get such effects in laboratory masers. Later interferometric observations (Rogers et al. 1966; Cudaback et al. 1966) implied brightness temperatures $> 2 \times 10^{60}$K; at such large intensities, maser emission is essentially required.

Some Motivation

We now know that many interstellar molecules are masing, in the sense that the observed line intensities are enhanced because the radiation has propagated through regions of negative optical depth and negative excitation temperature. Three molecules produce fairly strong emission lines in many sources: OH, H_2O, and SiO. These masers are particularly interesting because:

(1) They are fairly common astronomical objects. The number of type I OH masers in Turner's (as yet unpublished) survey is >150, more than the number of known pulsars. Also, Wilson and Barrett (1972) estimate that ~6% of all Mira

variables are type IIb OH masers. Since there are ~4600 Miras catalogued (see Allen 1973), that implies > 270 type IIb masers.

(2) They are found in a wide range of astrophysical conditions: dark dust clouds, dense molecular clouds, protostellar condensations, circumstellar regions of young stars, circumstellar envelopes of evolved stars, stellar remnants.

(3) They seem to involve rather sophisticated physics. In particular, people who study the origin of OH maser polarization find themselves worrying about fundamental details of the interaction of strong radiation with matter.

(4) They provide information about unique regions. The excitation of many maser transitions (H_2O, excited OH, SiO) requires high densities and temperatures. (One would have expected to be able to study such regions only with presently unobservable far-infrared transitions.) The high intensities enable the study of regions of small angular size: e.g., a 1 au source at 1 kpc suffers a dilution factor of 4×10^{-10} when observed at 1.35 cm with a 100-m telescope; in order to be detectable at the 0.1°K level, it must have a brightness temperature of 2.5×10^{8}°K.

(I.e., the only 1 au. sources that we could expect to detect are masers.)

Spectroscopic Structure of the Important Masers

SiO is a simple diatomic molecule. It can be pictured as two nuclei embedded in a cloud of electrons. Each nucleus feels the electrostatic attraction of the electron cloud and the electrostatic repulsion of the other nucleus. The resulting potential of the ground state, as a function of the distance between nuclei, is:

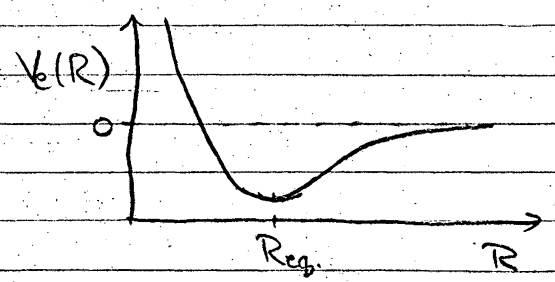

For small $|R-R_{eq}|$, $V(R)$ looks like a harmonic oscillator potential, so there is a sequence of vibrational energy levels. In addition, there are end-over-end rotational motions, with energies small compared to the vibrational energies. The rotational motions can thus be considered to be superimposed on each vibrational state. The resulting energy level scheme is shown in figure 1. The masing transitions are $v=1$, $J=3\to2$, $2\to1$, $1\to0$ and $v=2$, $J=1\to0$.

H_2O is an asymmetric molecule, with three unequal moments of inertia, so its rotational energy level structure is much more complex. Fortunately, it is only observed in the $v=0$ state. Some of the energy levels are shown in figure 2. The masing transition is $6_{16} \rightarrow 5_{23}$.

OH is a diatomic molecule, so it has a simple rotational spectrum. But the rotational transitions are in the far infrared (the first is at 120μ). The radio-frequency transitions arise from more subtle interactions: (i) spin-orbit interaction splits the energy level structure into two rotational ladders, $^2\Pi_{3/2}$ and $^2\Pi_{1/2}$; (ii) Λ-doubling splits each rotational state into states of opposite parity; (iii) hyperfine interaction splits each Λ-doublet state into two states of different total angular momentum. The transitions observed in maser emission, marked on figure 3, are: $^2\Pi_{3/2}$, $J=3/2$, $2\rightarrow2$, $1\rightarrow1$, $2\rightarrow1$, $1\rightarrow2$; $^2\Pi_{3/2}$, $J=5/2$, $3\rightarrow3$, $2\rightarrow2$; $^2\Pi_{3/2}$, $J=7/2$, $4\rightarrow4$; and $^2\Pi_{1/2}$, $J=1/2$, $1\rightarrow0$, $0\rightarrow1$.

Like H_2O, CH_3OH is too complicated to believe. The suspected maser transitions are marked on figure 4.

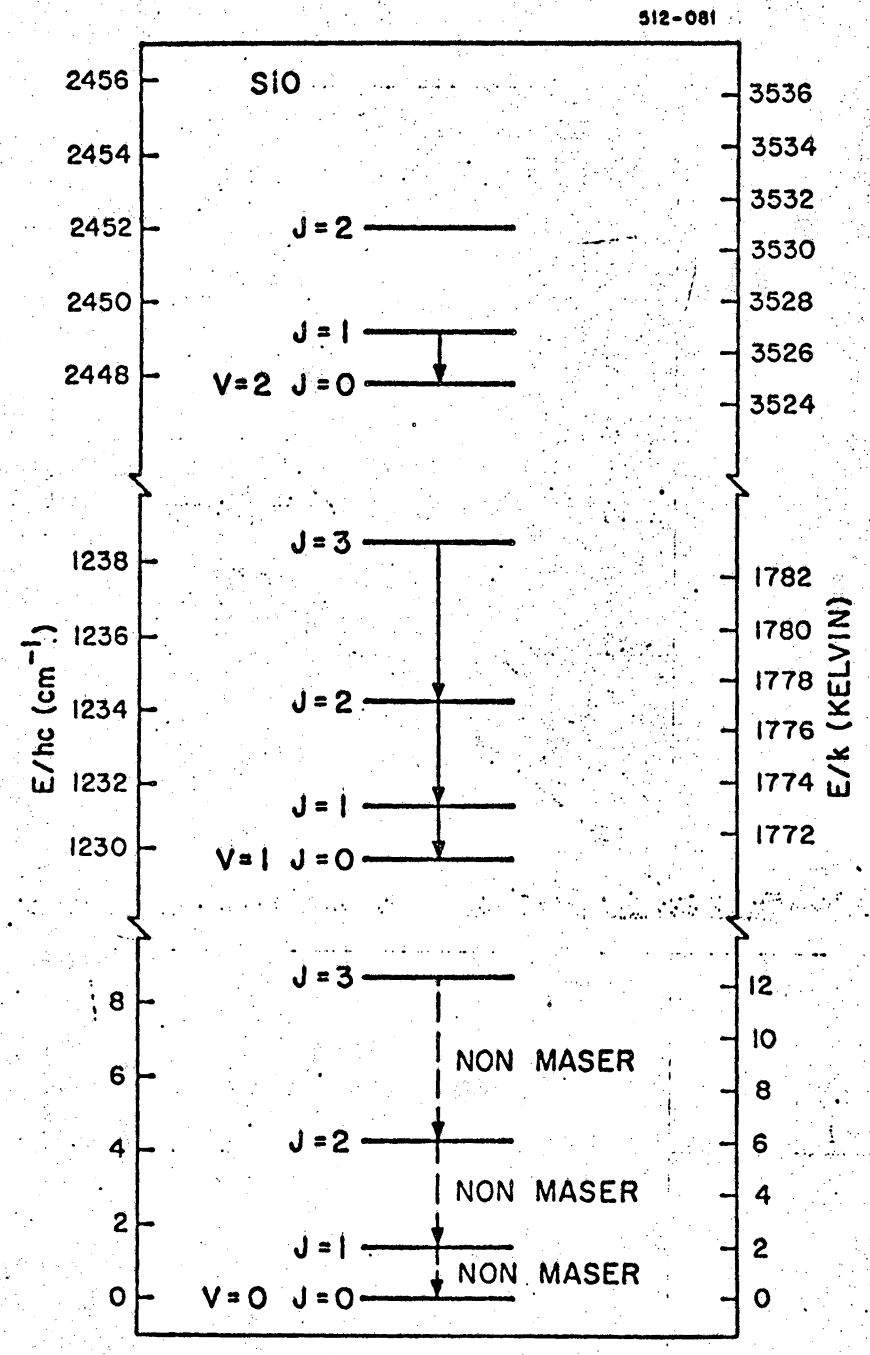

Moran, figure 8

1

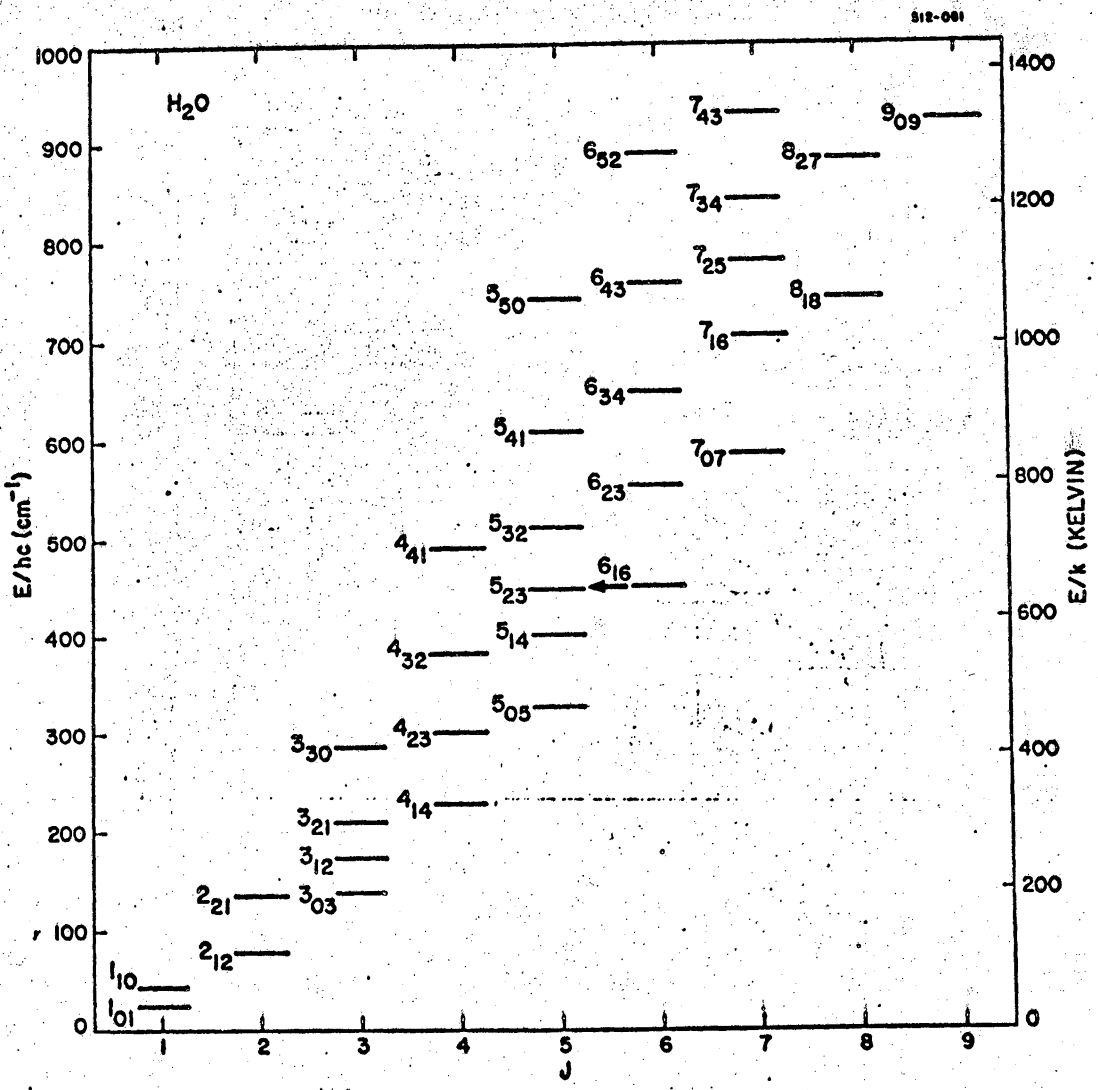

Moran, figure 10

2

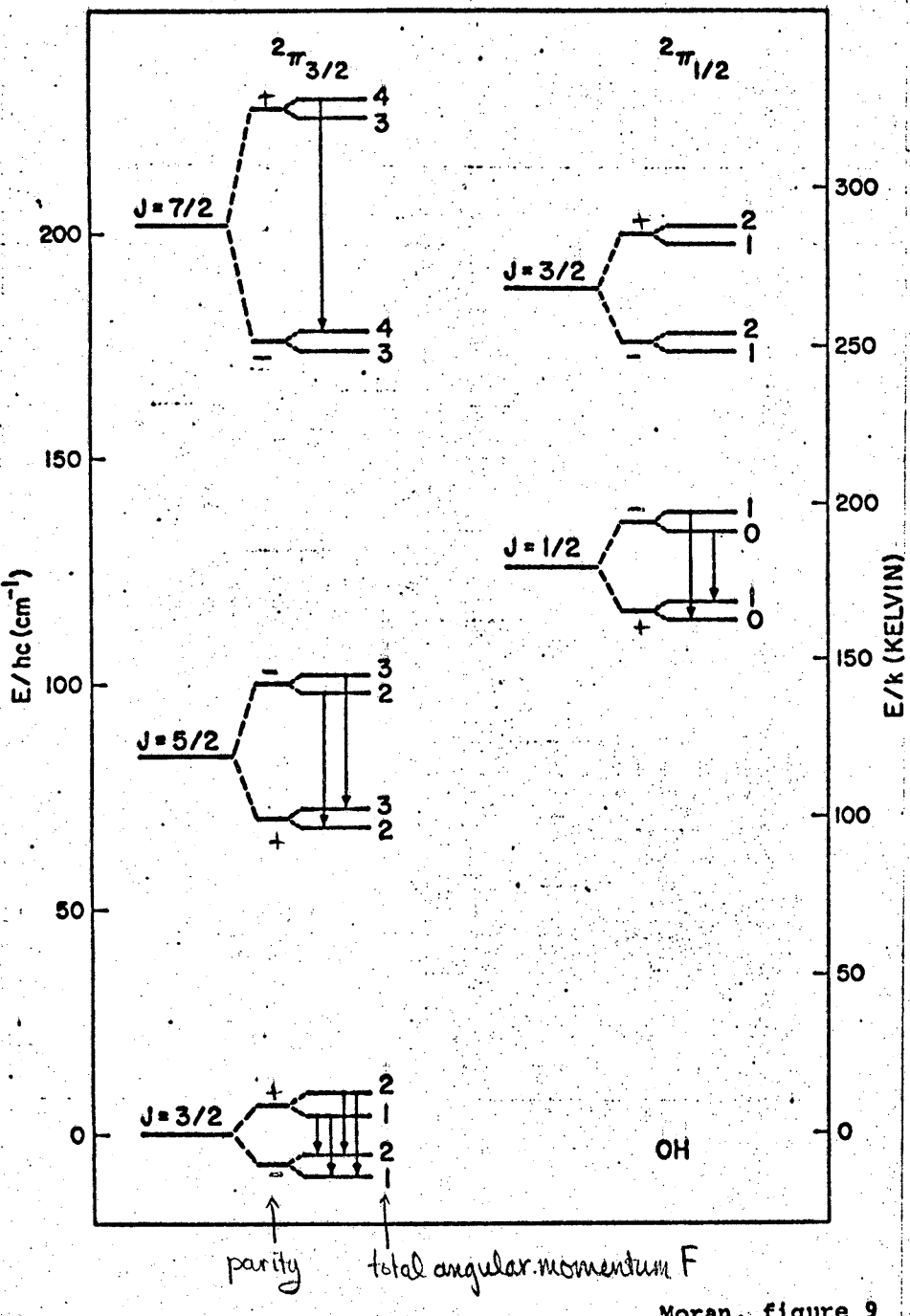

Moran, figure 9

3

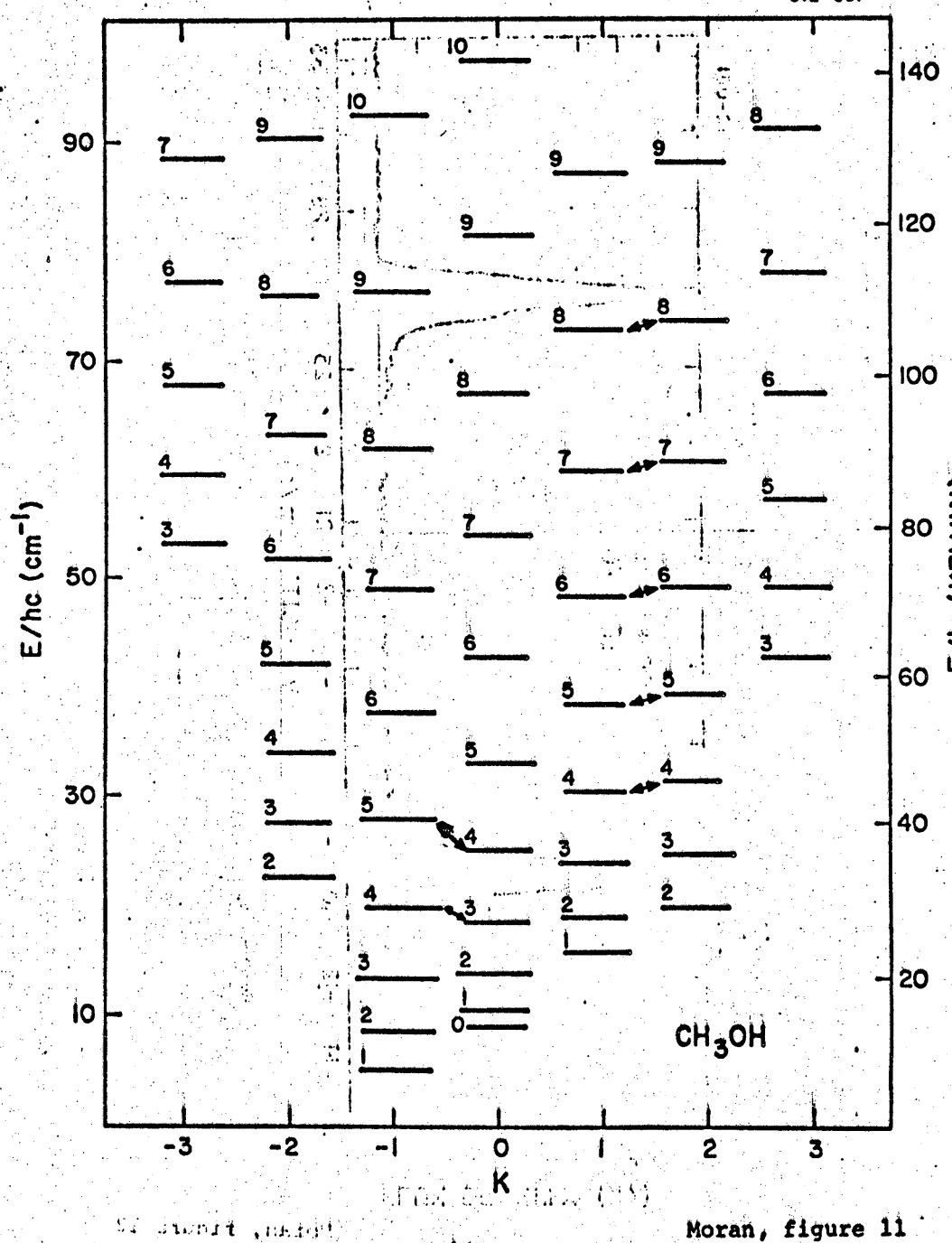

Moran, figure 11

4

Two Main Types of Maser Sources

A) HII Region masers.

These were first distinguished by their ground-state OH emission characteristics, Turner (1970) type I: there is strong emission at 1665 and 1667 MHz, with the 1665 lines almost always stronger than the 1667 lines. Emission at 1612 or 1720 MHz is usually weak or nonexistent. The OH spectra generally show many features with widths ~0.1 to 1.0 km/s spread over a range $\lesssim$ 20 km/s. There are almost never any obvious velocity correspondences between transitions. The features are usually circularly polarized, perhaps as much as 100%; linear polarization is also seen, but much less often. Some features vary on timescales $\gtrsim$ months. A typical spectrum, W3(OH), is shown in figure 5.

The strongest type I sources also have rotationally-excited OH masers, generally showing fewer velocity features. Circular and linear polarization are seen, as are slow time variations. A few rapid variations, with timescales ~ 1 day, have also been observed.

Most type I OH masers, when checked to a sufficiently low level, are also found to be H_2O masers. The H_2O spectra are

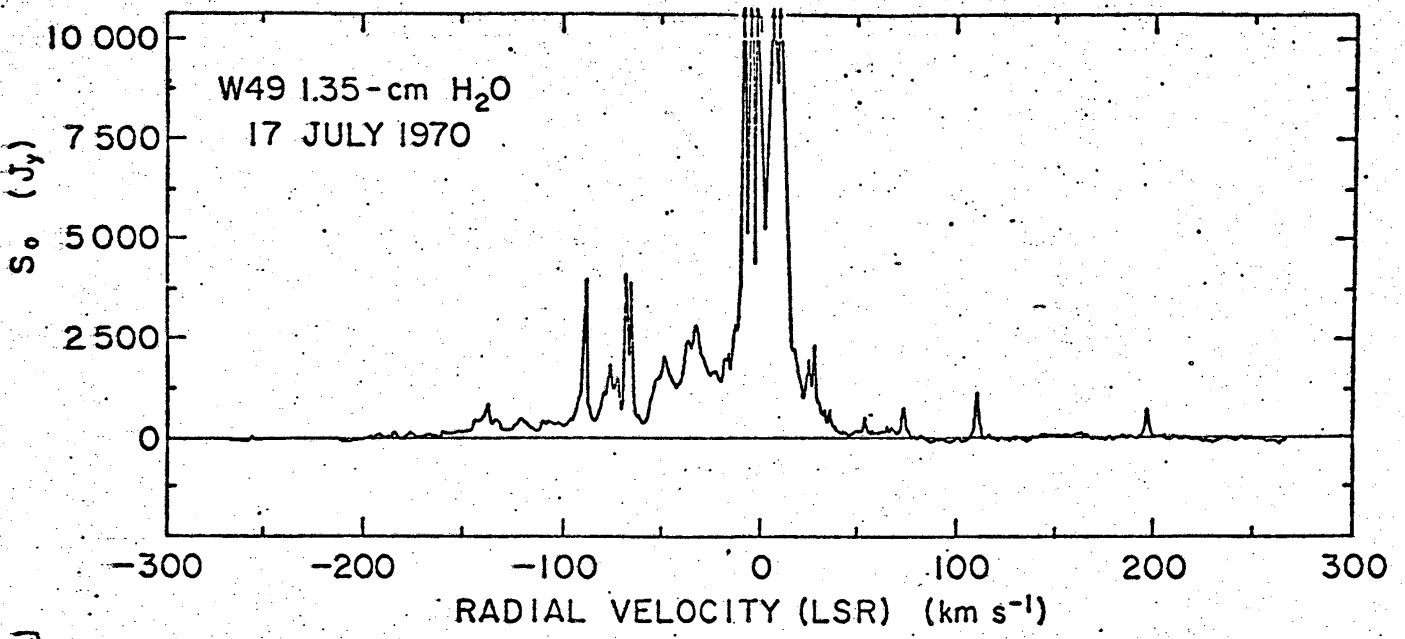

Fig. 1

Heckman, T.M., + Sullivan, W.T., III 1976, Ap. Letters,

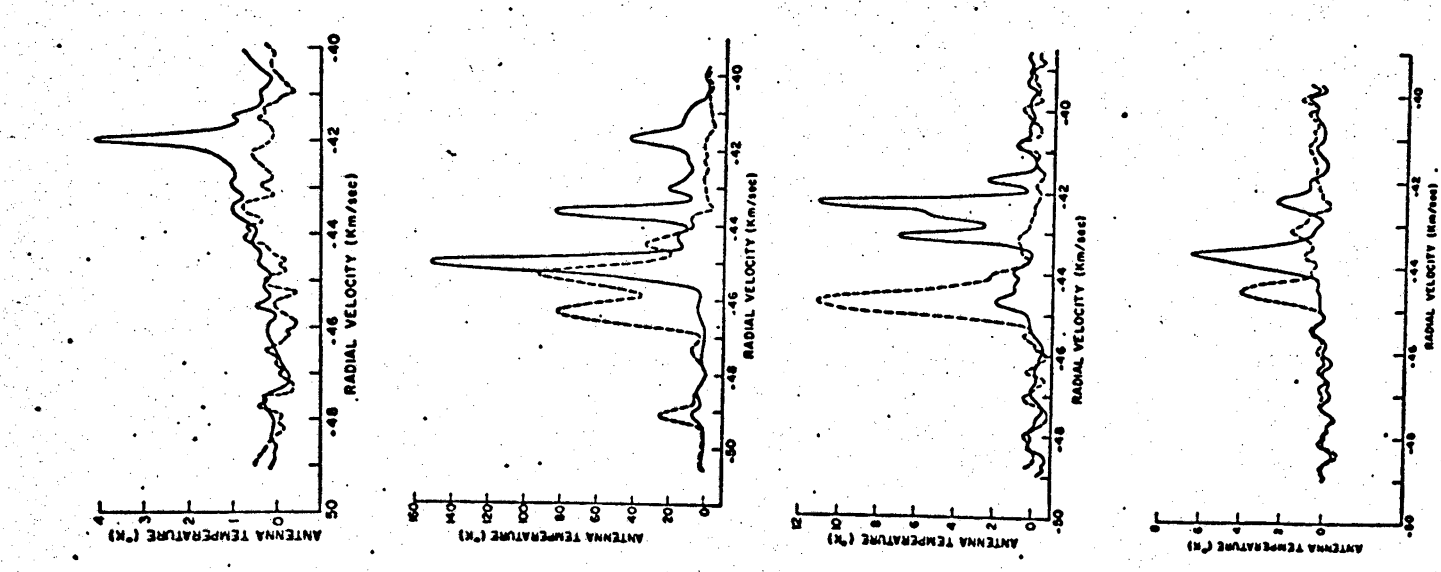

Moran, figure 16

often very complex, occasionally showing features over a wide velocity range (>300 km/s). An example, W49, is shown in figure 6. The H_2O features are never circularly polarized, but are often linearly polarized by as much as 40%. Individual features are often variable, with timescales as short as days. There is some evidence that the % of polarization of particular features can also vary.

When observed with an interferometer, both OH and H_2O emission features are found to arise from small spots distributed through a larger region (see figure 7). Each spot corresponds to a different velocity feature. The OH spots have diameters $\sim 10^{14}$ cm, the H_2O spots $\sim 10^{13}$ cm. Both are distributed over regions of diameter $\sim 10^{16}$ cm but, in the few cases where the observations give accurate absolute positions, the OH and H_2O regions don't overlap. About half the time, the masers are found to be near (but not coincident with) compact HII regions (continuum knots ~0.1 to 0.01 pc in size, with $n_e \sim 10^{5-6}$ cm^{-3}). (For W3(OH), it is possible that the OH spots are in a shell around the compact HII region.) Again about half the time, the masers are also associated with compact infrared

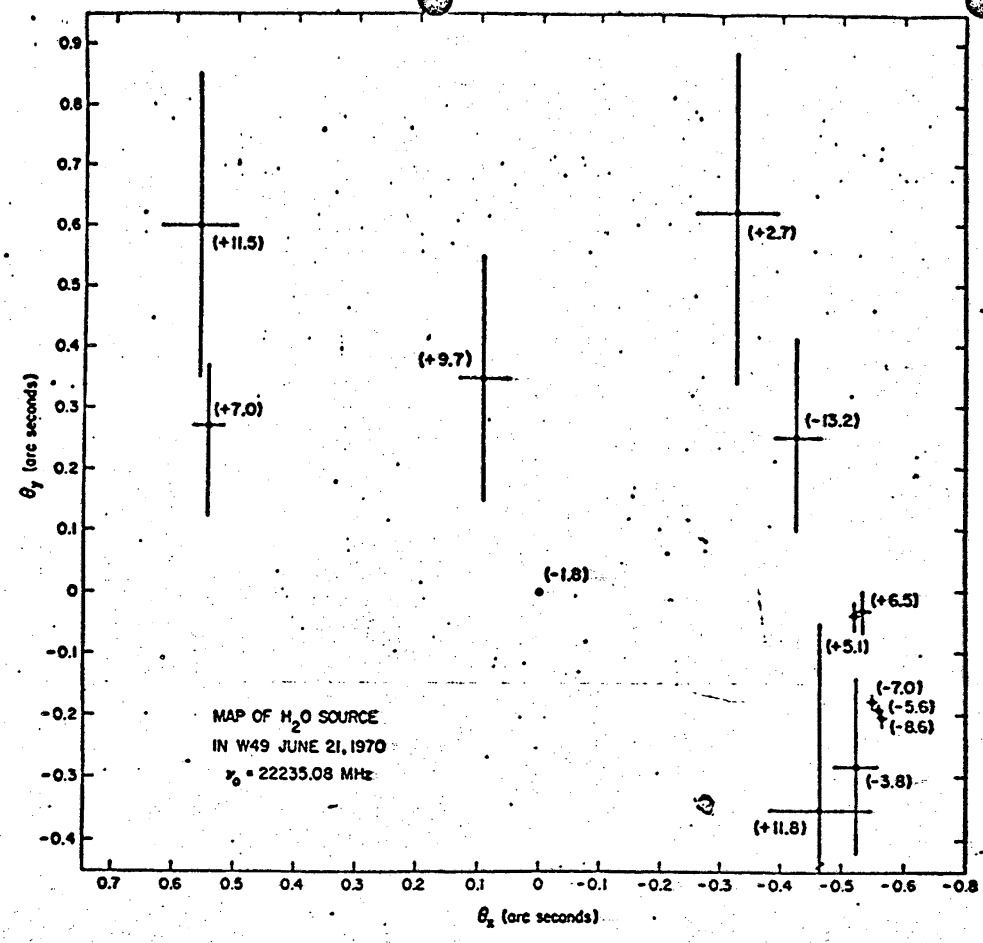

Moran, Figure 2

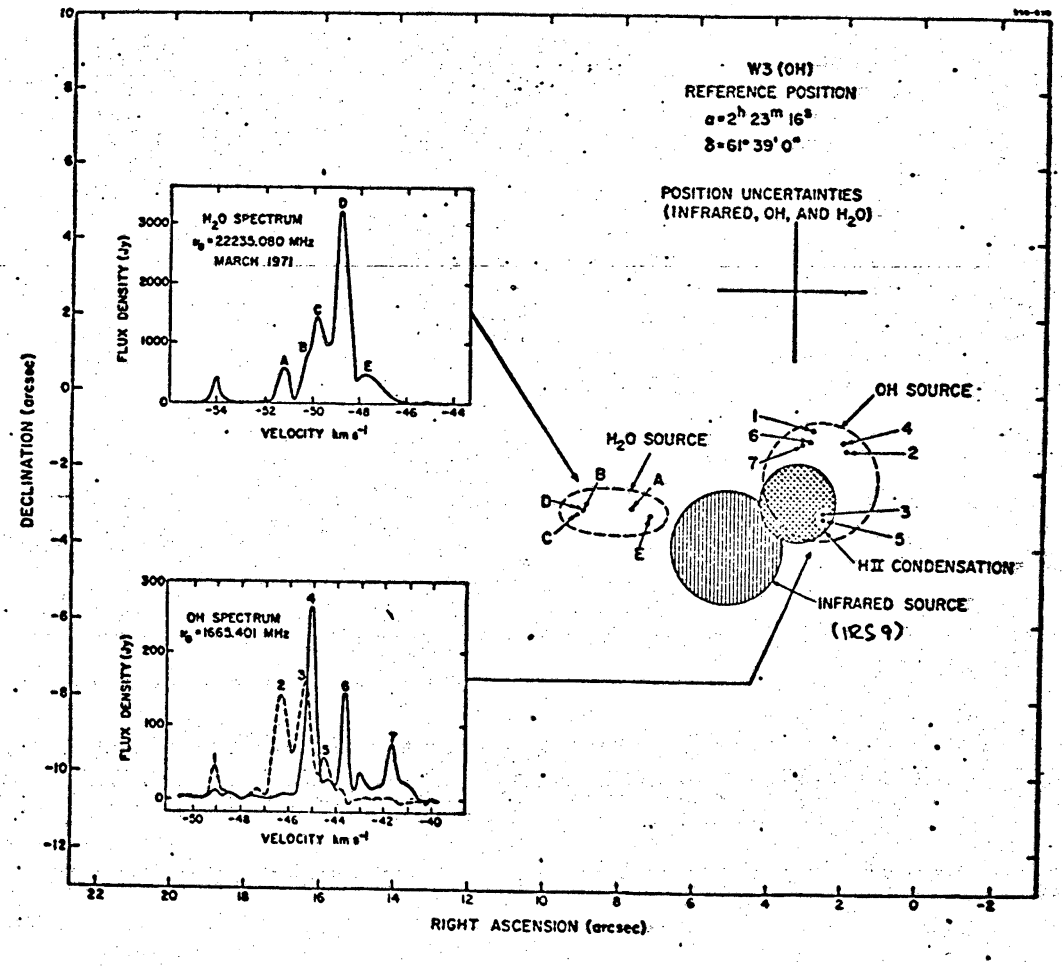

Moran, Figure 17

sources (see figure 8).

If the source sizes are as measured by the interferometers (cf. below), they imply $T_B(OH) = 10^{12-13}$ °K, $L(OH) = 10^{25-29}$ erg/s, $T_B(H_2O) = 10^{13-15}$ °K, $L(H_2O) = 10^{28-32}$ erg/s. Note that these figures refer to individual velocity features.

Arguing from the statistics of type I OH/H_2O masers (association with HII, IR; sizes and luminosities; pump models [discussed later]; etc.) a general picture of the evolution of HII region masers has been sketched by some authors (e.g., Lo 1975, Habing et al. 1974): A massive star forms within a dense dust cocoon. The heated dust pumps maser emission in the surrounding H_2O. As the star's UV radiation ionizes the cocoon (to form a detectable compact HII region), it dissociates the H_2O, producing OH which is also pumped into maser emission. The HII region grows and eventually (after $\sim 10^4$ yr) destroys the OH as well. This picture leaves many questions unanswered.

B) Circumstellar masers

These were also first distinguished by their ground-state OH properties, Turner (1970) type IIb: strong emission at 1612 MHz occasionally weaker emission at 1665 and 1667 MHz, and no

1720 MHz emission. The 1612 MHz emission usually has a distinctive line shape,

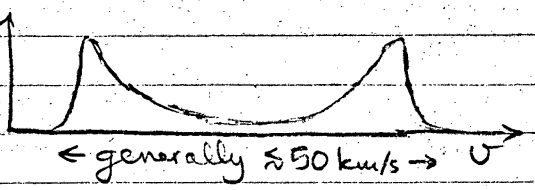

and is usually unpolarized

Most type II b OH masers also show H_2O maser emissions, and ~20% have SiO maser emission. The H_2O and SiO features generally fall at velocities within the OH pattern.

These masers are associated with late-type stars that have strong near-IR excesses. These are generally Mira variables or irregular supergiant variables with oxygen-rich atmospheres, and total luminosities $\sim 10^4 L_\odot$. typical effective temperatures ~1800–2800° K. The strong emission over 3–20 μ implies the presence of a dust shell with a temperature ~600–800° K. The stellar velocities are probably within the OH pattern, but its difficult to determine.

Interferometer maps have been made for a few sources; they again show small spots. The OH spots have diameters $\sim 10^{15}$ cm (luminosities $\sim 10^{24-28}$ erg/s) and are distributed over a region of size $\sim 3 \times 10^{16}$ cm. The H_2O spots have diameters $\sim 10^{14}$ cm (luminosities $\sim 10^{24-28}$ erg/s) and are distributed over $\sim 10^{15}$ cm.

The type II b masers are often variable, but in a manner different from the HII region masers. The OH and H_2O flux varies in a

rough sinousoidal fashion as does the infrared. The periods are 10^{2-3} days long, and the maser maxima lag the IR maxima by ~0.1–0.2 periods. This is interpreted as radiative coupling between the stellar flux and the maser, presumably through the pumping mechanism.

The Elitzur et al. (1974) model is fairly typical among those proposed for type II b masers. The stellar mass loss includes dust and H_2O. The dust is heated by the star, and radiates at 6μ, exciting the H_2O, $v=0\to1$ transition and pumping the H_2O maser. As the circumstellar cloud flows outward, the ambient interstellar UV field dissociates the H_2O, producing OH, which is also pumped by the near-IR emission of the dust. In other models (e.g., Harvey et al. 1974, Schwartz et al. 1974), there is a similar configuration, but the molecules are pumped directly by stellar radiation.

Basic Radiative Transfer for Masers

Consider the energy levels of some maser transition,

2 ———

1 ———

connected to other (unspecified) energy levels (including continuum states) in unspecified ways.

Statistical equilibrium:

$$\frac{dn_1}{dt} = An_2 + B_{21}In_2 - B_{12}In_1 + C_{21}n_2 - C_{12}n_1 + P_1N - \Gamma_1 n_1$$

$$\frac{dn_2}{dt} = \underbrace{B_{12}In_1 - An_2 - B_{21}In_2}_{\text{Radiative transitions between levels 1 \& 2.}} \underbrace{+ C_{12}n_1 - C_{21}n_2}_{\text{Collisional transitions between 1 \& 2}} \underbrace{+ P_2N}_{\text{All input from other levels}} \underbrace{- \Gamma_2 n_2}_{\text{All outflow to other levels.}}$$

Here $N = n_1 + n_2$ is proportional to the total number of masing molecules.

Assuming steady state: $\frac{dn_1}{dt} = \frac{dn_2}{dt} = 0$, and after tedious algebra,

$$\Delta n \equiv n_2 - n_1 = N \frac{(P_2 - P_1) + \frac{1}{2}(\Gamma_1 - \Gamma_2) - [A + B_{21}I - B_{12}I] - [C_{21} - C_{12}]}{(A + B_{21}I + B_{12}I) + (C_{21} + C_{12}) + \frac{1}{2}(\Gamma_1 + \Gamma_2)}$$

For $\Delta n > 0$, the energy level populations are inverted, and we have a maser.

Let $\Delta W_r = A + B_{21}I - B_{12}I$, $\Delta W_c = C_{21} - C_{12}$ $(\Delta W_r, \Delta W_c \geq 0)$

$W_{rt} = A + B_{21}I + B_{12}I$, $W_{ct} = C_{21} + C_{12}$

$$\Delta n = N \frac{(P_2 - P_1) + \frac{1}{2}(\Gamma_1 - \Gamma_2) - \Delta W_r - \Delta W_c}{W_{rt} + W_{ct} + \frac{1}{2}(\Gamma_1 + \Gamma_2)}$$

Note that if levels 1 and 2 are the only energy levels of the molecule ($P_1 = P_2 = \Gamma_1 = \Gamma_2 = 0$), then Δn is always ≤ 0; i.e. we can never have a maser. This is just a consequence of the 2nd Law of Thermodynamics. The two levels have a unique temperature (Tex) that you can change by connecting up with various reservoirs (radiation fields, colliding molecules, etc.) at various temperatures. But you can never cool Tex below the temperature of the coolest reservoir which, for the physical situations available, will be > 0.

For convenience, let $P_{eff} \equiv (P_2 - P_1) + \frac{1}{2}(\Gamma_1 - \Gamma_2) - \Delta W_r - \Delta W_c$ (the effective pump rate). Furthermore, assume equal statistical weights for the 2 levels ($B_{12} = B_{21}$) and a rectangular line of width $\Delta\nu$. The one-dimensional equation of transfer becomes:

$$\frac{dI}{dx} = \frac{h\nu}{4\pi\Delta\nu}\left[\Delta n B I + n_2 A\right]$$

$$= I\frac{h\nu B}{4\pi\Delta\nu}\frac{NP_{eff}}{W_{ct} + A + \frac{1}{2}(\Gamma_1+\Gamma_2)}\frac{1}{1 + \frac{2BI}{W_{ct}+A+\frac{1}{2}(\Gamma_1+\Gamma_2)}} + \frac{h\nu n_2 A}{4\pi\Delta\nu}$$

$$= \frac{\alpha_0 I}{1 + I/I_s} + \epsilon$$

Note that $\alpha_0 I = \frac{h\nu}{8\pi\Delta\nu} NP_{eff}\frac{I}{I_s}$ and $\Delta n = \frac{(NP_{eff}/2BI_s)}{1 + I/I_s}$

We can isolate two regimes:

A) Unsaturated amplification : $I/I_s \ll 1$

Here $\frac{dI}{dx} \simeq \alpha_0 I + \epsilon$, so $I(x) = I(0)e^{\alpha_0 x} + \frac{\epsilon}{\alpha_0}(e^{\alpha_0 x} - 1)$

For $\alpha_0 x$ small, $I(x) \simeq I(0) + \epsilon x$ (linear growth)

As $\alpha_0 x$ becomes larger, $I(x) \simeq \left(I(0) + \frac{\epsilon}{\alpha_0}\right)e^{\alpha_0 x}$ (exponential growth)

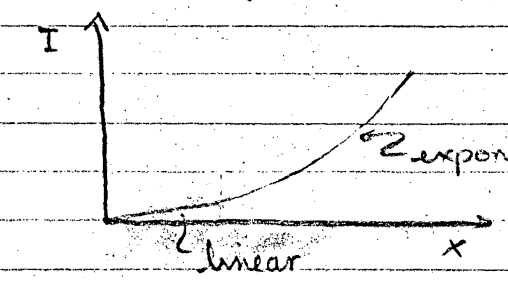

For total pathlength L through the region of inversion, the initial

radiation field is amplified by $\sim e^G$, $G = \alpha_0 L$ = gain.

Note that $\Delta n \simeq \frac{NP_{eff}}{2BI_s}$, so that the inversion is completely controlled by the pumping mechanism.

B) Saturated amplification: $I/I_s \gg 1$.

Here $\frac{dI}{dx} \simeq \alpha_0 I_s + \epsilon$, so $I(x) = I(0) + \alpha_0 I_s x + \epsilon x$ (linear growth)

Note that $\Delta n \simeq \frac{NP_{eff}}{2BI}$. The radiation field is beginning to compete with the pump, trying to destroy the inversion by stimulating the 2→1 transition.

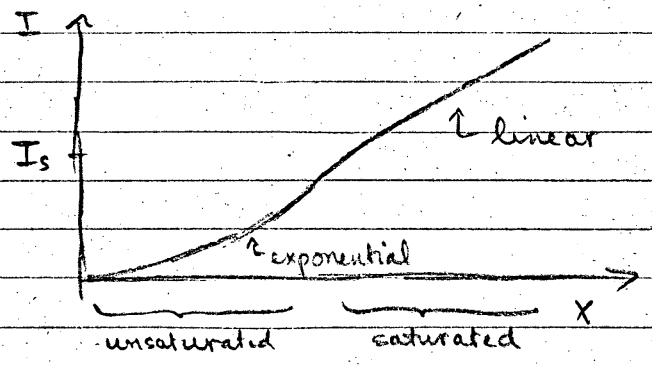

We can look at this another way: at $I = I_s$,

$$\frac{dI}{dx} = \frac{1}{2}\alpha_0 I + \epsilon = \frac{h\nu}{16\pi\Delta\nu} NP_{eff} + \epsilon$$

Neglecting ϵ (which is small compared to I_s), this tells us that as the pump energy is put in, it is immediately converted into the energy of the radiation field (modulo a factor of $\frac{1}{4}$ at $I = I_s$), and can't be used to build up the inversion any more.

The distinction between these two regimes has observable effects.

i) Line narrowing

Suppose the initial radiation had a Doppler profile:

$$N = N(\nu) = N_0 \exp\left[-4\ln 2 \frac{(\nu-\nu_0)^2}{\Delta\nu^2}\right]$$

If you plug this into the unsaturated maser equation, the resulting profile is roughly Gaussian, but with width

$$\Delta\nu' \simeq \frac{\Delta\nu}{\sqrt{G_0}}, \quad G_0 = \alpha_0(\nu=\nu_0)X$$

The stronger parts of the line (the center) are amplified more $\left(\frac{dI}{dx} \propto I\right)$, so the line narrows. For $G_0 \sim 25$, you can make a line with a Doppler width corresponding to 10^3°K look like a line of Doppler width corresponding to <50°K.

But if the maser is saturated, the line core grows linearly while the line wings (still unsaturated) grow exponentially, and catch up. For a strongly saturated maser, the line is broadened out to its original width. [However, Goldreich and Kwan (1974a) have a mechanism that will keep the line from broadening in saturated masers.]

ii) Time variations

Neglecting ϵ, $I = I_0 e^G$ for an unsaturated maser, so $\delta I = I_0 e^G \delta G$, i.e. $\frac{\delta I}{I} = \delta G$; a 1% change in G produces a 6% change in I.

For a saturated maser, though, $I = I_0 + G I_s$, $\delta I = I_s \delta G$, and

$$\frac{\delta I}{I} = \frac{I_s \delta G}{I_0 + G I_s} = \frac{\delta G}{G} \frac{1}{1 + I_0/I_s G} \leq \frac{\delta G}{G};$$ a 1% change in G produces <u>at most</u> a 1% change in I.

iii) Apparent source size (a rough description)

Consider two path lengths through a spherical maser of diameter D. The path through the diameter has length D, the chord has length $D\sqrt{1 - 4y^2/D^2}$, so $\frac{G(y)}{G(0)} = \sqrt{1 - 4y^2/D^2}$

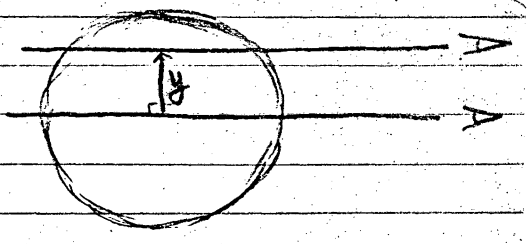

and $\frac{I(y)}{I(0)} \propto \exp\left[G_0\sqrt{1 - 4y^2/D^2}\right]$. Thus the apparent source size, D^*, will be smaller than the true source size D: $\frac{D^*}{D} \simeq \frac{1}{\sqrt{G_0}}$.

As G_0 increases, the apparent source size decreases. Eventually, G_0 is sufficiently high so that the intensity at the surface of radiation moving along the diameters (not necessary toward the observer) saturates the edge. A line of sight through the saturated edge shows only linearly amplified background radiation and spontaneous emission.

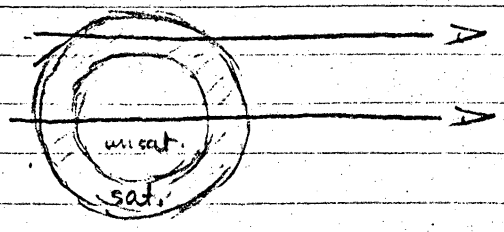

The saturated edge is essentially invisible in comparison with the unsaturated core. So D^* is further reduced.

When the maser becomes saturated throughout, the apparent size increases again, because $\frac{I(y)}{I(0)} = \sqrt{1 - 4y^2/D^2}$.

In this limit, $\frac{D^*}{D} = \frac{\sqrt{3}}{2}$.

Also note: because the gains decrease for directions away from the diameter, the radiation in any particular direction becomes strongly beamed. (hence the source size effect). So at the cloud surface, the radiation field is very anisotropic. We ignored this in the equation of transfer. In fact, it may be a very important effect.

iv) Statistics.

For simple spontaneous emission, the observed radiation arrives with random phases, and the total electric field amplitude observed at a given instant of time is an average over these different phases. Because of the large number of sources, the probability of observing some amplitude $|\vec{E}|$ is Gaussian distributed:

$$P(|\vec{E}|) = \frac{1}{\sqrt{2\pi}} \exp\left\{-\frac{|E|^2}{2\sigma^2}\right\}.$$

In a laboratory maser with feedback, the phases are all aligned, because the radiation is essentially all stimulated emission & thus has the same phase and direction as the stimulating radiation.

Astrophysical masers are intermediate. For an unsaturated maser, you expect Gaussian statistics because the maser is amplifying the random phase distribution of the incident

radiation field or the internal spontaneous emission. But with the onset of saturation, there are nonlinear effects: the gain is smaller for signals with stronger $|\vec{E}|$. So the probability of observing the larger values of $|\vec{E}|$ is decreased below the Gaussian value.

So, are interstellar masers saturated or unsaturated? There are some tests:

(i) Measure I (i.e., T_B) and compare it with I_s. Doing so, it turns out that the smallest sources (small H_2O spots) are just barely saturated. Since we expect that the physical sizes are even larger, it seems likely that all OH & H_2O masers are saturated.

(ii) Sources often show several velocity components with comparable intensities. If the sources were unsaturated, small differences in G would mean large differences in I, and we wouldn't expect so many sources to have similar intensities.

(iii) Look at the statistics. Evans et al. (1972) did so, and found no detectable deviation from Gaussian statistics. This would suggest unsaturated masers, but:

(a) scattering of signals by the intervening interstellar medium may wash out expected deviations, and

(b) even with interferometers, we may be averaging over many regions of (different) constant phase.

[We can define a correlation length $\frac{\eta_{\pi\Delta\nu}}{h\nu B n_{OH}} = \frac{\delta\tau_1 \Delta\nu}{\lambda^2 A n_{OH}} \sim 2\times10^{11}$ cm, for $A \sim 10^{-10}$ s; $n_{OH} \sim 10$ cm^{-3}. This implies a constant phase area $\sim 4\times10^{22}$ cm^2, vs. a spot area $\gtrsim 10^{26}$ cm^2. So there's room for more than 200 phase patches, quite enough to produce Gaussian statistics via the central limit theorem.]

Pump Models

There are many OH, H_2O, and SiO pump models; were we to discuss the advantages and disadvantages of each, these notes would rapidly become tedious. So we shall concentrate on general pump theory, especially thermodynamics.

Consider these simple three-level pumps. W_{13} and W_{32} correspond to energy reservoirs at different temperatures.

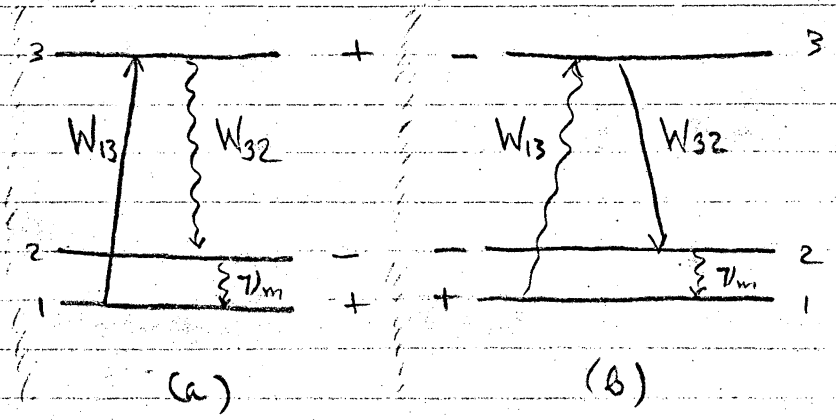

a) W_{13} : collisions with H_2 molecules at high $T_{kinetic}$
W_{32} : radiation into a field w/ $T_{rad} \ll T_{kin}$ (e.g. 3°K background)

b) W_{13} : radiative excitation by field at high T_R (e.g. IR from hot dust)
W_{32} : collisional deexcitation by H_2 molecules at low T_{kin}

Using the Boltzmann formula and writing $\frac{n_2}{n_1} = \frac{n_3/n_1}{n_3/n_2}$, we derive:

i) an approximate relation: $\frac{1}{T_{32}} - \frac{1}{T_{31}} \simeq -\frac{1}{T_{21}} \frac{\nu_m}{\nu_p}$,

where T_{32}, T_{31}, and T_{21} are the excitation temperatures of the 3 pairs of levels and $\nu_{32} \simeq \nu_{13} = \nu_p$. So to get inversion ($T_{21} < 0$), we need $T_{31} > T_{32}$, as written for examples (a) and (b). (ν_m/ν_p) represents the efficiency of energy transfer between pump and maser, η_m.

ii) more carefully: $\frac{n_2}{n_1} = \exp\left[\frac{h\nu_m}{kT_{32}}\left(\underbrace{\frac{\nu_p}{\nu_m}}_{(\eta_m)^{-1}} \underbrace{\frac{T_{31}-T_{32}}{T_{31}}}_{\eta_c} - 1\right)\right]$

(cf. Scovil et al. 1959).

η_c is just the efficiency of the Carnot cycle describing the pump process. For inversion ($\frac{n_2}{n_1} > 1$) we must have $\eta_m \leq \eta_c$.

So the maser is almost never as efficient as the pump. Furthermore the most efficient maser is one that is very saturated ($\frac{n_2}{n_1} \to 1$).

The presence of a radiative transition in the pump cycle leads to a constraint on the process. If the optical depth in the radiative transition becomes large, the radiation field in the

line is thermalized to the kinetic temperature; i.e. $T_{32} \simeq T_{31}$, and we can't sustain an inversion. The resulting constraint is that the rate of photon leakage in the line be sufficiently fast (at least as fast as the maser transition rate). The maximum leakage rate is $\Lambda_{max} = \rho \frac{c\Delta\nu}{4\pi h\nu} 4\pi r_{cloud}^2$, $\rho = \frac{8\pi h\nu^3/c^3}{e^{h\nu/kT_B} - 1}$, T_B = line brightness temperature. This often turns out to be a crucial factor in the ability of a hypothetical pump to work in a real cloud. For example, the -3.5 km/s H_2O feature in W49 (very famous because $L_{H_2O} \sim 1 L_\odot$) radiates $\sim 5\times10^{46}$ photons/s, and has an apparent size $\sim 3\times10^{13}$ cm. If the radiative part of the pump falls at $\sim 100\mu$, w/ $T_B \sim 500°K$ and $\Delta\nu/\nu \sim 7\times10^{-6}$ (typical values from a far-IR pump model), $\Lambda_{max} \sim 5\times10^{40}$ photons/s. This misses having maser rate $\leq$ leakage rate by a factor of 10^8. We can try to get around this by invoking the fact that the physical cloud size is larger than the apparent one, but we'd need $D^*/D \sim 10^{-4}$ (quite unlikely).

The usual way that people get around this is by distributing the radiation source (or sink) throughout the masing material. Consider, e.g., the Goldreich and Kwan (1974b) H_2O pump. Dust is heated by a continuum source (UV from an HII region,

near-IR from a star) and emits strongly in the near infrared. It emits strongly at 6μ, exciting nearby H_2O to the $v=1$ state. The excited H_2O is collisionally deexcited by cool H_2 molecules ($T_{gas} < T_{dust}$), and the $6_{16}-5_{23}$ transition ends up being inverted. Both the pump (hot dust radiation) and the sink (cool gas collisions) are mixed with the masing H_2O, so the optical depths can be kept low. Providing that the timescale for collisional equilibration of T_{gas} and T_{dust} is long enough, Goldreich and Kwan can get a maser.

The Elitzur et al. (1976) 1612 MHz maser pump is similar. Warm dust grains excite the $^2\Pi_{3/2}, J=3/2 \rightarrow {}^2\Pi_{1/2}, J=5/2$ transition at 35μ. The excited states radiatively decay, with small optical depths for the most part. The details of the decay from $^2\Pi_{1/2}, J=1/2$ to $^2\Pi_{3/2}, J=3/2$ leads to an inversion of the hyperfine levels within each Λ-doublet state, sufficient to bring about a 1612 MHz inversion. The pump is again distributed through the maser. We do have to worry about the leakage rate in the (optically-thick) $^2\Pi_{1/2}, J=1/2 \rightarrow {}^2\Pi_{3/2}, J=3/2$ transitions, but it turns out to be sufficiently fast to explain even the strongest IR star masers.

The Gwinn et al. (1973) pump for type I OH masers is similar to example (a). OH is produced in highly-excited states by collisions with H or H_2 or by the collisional dissociation of H_2O. The excited-OH decays down the rotational ladder and, because of subtle quantum-mechanical details of the collision process, preferentially populates the upper Λ-doublet levels in the $^2\Pi_{3/2}$ ladder. Again, the pump is distributed through the maser, but the sink (radiative deexcitation of rotational transitions) involves the leakage of photons out of the cloud in optically-thick lines. It turns out that the leakage rate is just fast enough to account for the strongest OH line known in W49 (the strongest source). Maybe we don't see stronger lines because of these thermodynamic considerations.

Other Masers

A) Millimeter-wavelength methanol (CH_3OH)

Barrett et al. (1971) observed a set of lines in Orion (the 4_2-4_1, 5_2-5_1, 6_2-6_1, 7_2-7_1, 8_2-8_1 (E) transitions) for which the source size was <1′ (implying moderate T_B). From the relative intensities of the lines, they concluded that departures from LTE were not likely to be important. But Zuckerman

et al. (1972) and Turner et al. (1972) argued that the intensities of those lines relative to other methanol lines were quite anomalous. From statistical equilibrium calculations, they inferred that the lines were weakly masing. Chui et al. (1974) reobserved the $7_2 \rightarrow 7_1$ and $6_2 \rightarrow 6_1$ lines, finding them to be stronger than before. But, because the $(6_2-6_1)/(7_2-7_1)$ ratio hadn't changed, and because there were no variations during the 3 months of their observations (3 mo corresponds to the light-travel time of a 1'-diameter source at Orion), they decided that they were including another source within their larger beam. (Still, they noted that the only time variations in spectral lines in radio-astronomical sources were seen in masers.)

However, Hills et al. (1974) derived upper limits to the CH_3OH source size $\sim 10''-30''$, and also resolved the lines into several narrow (~ 0.4 km/s) features. Since T_B (implied by source size) >> T_K (implied by line width), they concluded that the lines were masing. They noted, though, that because the time variations were weak, T_B is probably not very large and, because of the similarity of the 6_2-6_1 and 7_2-7_1 line shapes, the overall gain is probably not too high.

B) Weak centimeter-wavelength masers

A number of large asymmetric-top molecules are observed in the direction of the galactic center sources SgrB2 and SgrA. Of these, NH_2CHO, $HCOOH$, CH_3CHO, CH_3OH (the 1, 1K-doublet), CH_3NH, CH_2CHCN, and possibly $HCOOCH_3$ are seen in weak emission against the very strong centimeter-wavelength continuum. [H_2CO and H_2CS absorption in the same direction, at the same velocity shows that (at least part of) the molecular cloud is in front of the continuum source.] But $T_A \simeq (T_{ex} - T_{background})\tau$, and it is very unlikely that $T_{ex} > T_{bg}$ [and it is certainly unlikely that $T_{ex} - T_{bg} = \delta > 0$ with the same δ for so many different molecules]. So Litvak (1973) and Gottlieb et al. (1973) infer that τ and T_{ex} are < 0 — i.e., these molecules are weakly masing.

REFERENCES

Review Articles

Goldreich, P. 1975, in Atomic and Molecular Physics and the Interstellar Medium, eds. R. Balian, P. Encrenaz, and J. Lequeux (Amsterdam: North-Holland), p. 409.

Kegel, W.H. 1975, in Problems in Stellar Atmospheres and Envelopes, eds. B. Baschek, W.H. Kegel, and G. Traving (Heidelberg: Springer-Verlag), p. 257.

Litvak, M.M. 1974, Ann. Rev. Astr. and Ap., 12, 97.

Moran, J.M. 1976, in Frontiers of Astrophysics (Harvard University Press) (soon to be published).

ter Haar, D., and Pelling, M.A. 1974, Repts. on Prog. in Phys., 37, 481.

Turner, B.E. 1970, R.A.S.C. Journal, 64, 221, 282.

Cited Articles

Allen, C.W. 1973. Astrophysical Quantities

Barrett, A.H., and Rogers, A.E.E. 1966, Nature, 210, 188.

Barrett, A.H., Schwartz, P.R., and Waters, J.W. 1971, Ap.J. (letters), 168, L101.

Chui, M.F., Cheung, A.C., Matsakis, D., Townes, C.H., and Cardiasmenos, A.G. 1974, Ap.J. (letters), 187, L19.

Cudaback, D.D., Read, R.B., and Rougoor, G.W. 1966, Phys Rev. Lett., 17, 452.

Davies, R.D., de Jager, G., and Verschuur, G. 1966, Nature, 209, 974.

Ehrenstein, G., Townes, C.H., and Stevenson, M.J. 1959, Phys Rev Lett, 3, 40.

Elitzur, M., Goldreich, P., and Scoville, N.Z. 1976, Ap.J., 205, 384.

Evans, N.J., Hills, R.E., Rydbeck, O.E.H., and Kollberg, E. 1972, Phys Rev A, 6, 1643.

Gardner, F.F., Robinson, B.J., Bolton, J.G., and van Damme, K.J. 1964, Phys Rev Lett, 13, 3.

Goldreich, P., and Kwan, J. 1974a, Ap.J., 190, 27.

———. 1974b, Ap.J., 191, 93.

Gottlieb, C.A., Palmer, P., Rickard, L.J, and Zuckerman, B. 1973, Ap.J., 182, 699.

Gundermann, E.J. 1965. Ph.D. thesis, Harvard University.

Gwinn, W.D., Turner, B.E., Goss, W.M., and Blackman, G.L. 1973, Ap.J., 179, 789.

Habing, H.J., Goss, W.M., Matthews, H.E., and Winnberg, A. 1974, Astr. and Ap., 35, 1.
Harvey, P.M., Bechis, K.P., Wilson, W.J., and Ball, J.A. 1974, Ap. J. Suppl., 27, 331.
Hills, R., Pankonin, V., and Landecker, T.L. 1975, Astr. and Ap., 39, 149.
Litvak, M.M. 1973, in Atoms and Molecules in Astrophysics, eds T.R. Carson and M.J. Roberts (New York: Academic), p. 201.
Lo, K.Y. 1974, Ph.D. thesis, M.I.T.
Rogers, A.E.E., Moran, J.M., Crowther, P.P., Burke, B.F., Meeks, M.L., Ball, J.A., and Hyde, G.M. 1966, Phys Rev. Lett., 17, 450.
Schwartz, P.R., Harvey, P.M., and Barrett, A.H. 1974, Ap. J., 187, 491.
Scovil, H.E.D., and Schulz-DuBois, E.O. 1959, Phys Rev Lett, 2, 262.
Shklovskii, I.S. 1949, Astr. Zhur., 26, 10.
Turner, B.E., Gordon, M.A., and Wrixon, G.T. 1972, Ap. J., 177, 609.
Weinreb, S., Barrett, A.H., Meeks, M.L., and Henry, J.C. 1963, Nature, 200, 829.
Weinreb, S., Meeks, M.L., Carter, J.C., Barrett, A.H., and Rogers, A.E.E. 1965, Nature, 208, 440.
Weaver, H., Williams, D.R.W., Dieter, N.H., and Lum, W.T. 1965, Nature, 208, 29.
Wilson, W.J., and Barrett, A.H. 1972, Astr. and Ap., 17, 385.
Zuckerman, B., Turner, B.E., Johnson, D.R., Palmer, P., and Morris, M. 1972, Ap. J., 177, 601.